

Flexible and Foldable Li–O₂ Battery Based on Paper-Ink Cathode

Qing-Chao Liu, Lin Li, Ji-Jing Xu, Zhi-Wen Chang, Dan Xu, Yan-Bin Yin, Xiao-Yang Yang, Tong Liu, Yin-Shan Jiang, Jun-Min Yan, and Xin-Bo Zhang*

The worldwide demand for flexible electronics continues to grow rapidly because of their favorable advantages in terms of being bendable, portable, rollable, and foldable,^[1–6] wherein high performance power device is a necessary key component. However, conventional energy storage/conversion devices are too bulky and rigid to be integrated into flexible electronics. In response, several inspirational prototypes, including flexible solar cells,^[7–10] rechargeable batteries,^[11–13] and supercapacitors,^[14–20] etc., have been developed. However, the low theoretical energy density of these new concept power devices would intrinsically limit their wide application in next-generation flexible devices. Fortunately, non-aqueous Li–O₂ batteries have been developed due to its extremely high energy density, 3600 Wh kg^{−1} (2Li⁺ + O₂ + 2e[−] ⇌ Li₂O₂, 2.96 V vs Li/Li⁺), which is nearly 10 times that of conventional lithium-ion batteries.^[21–32] Therefore, the development of flexible Li–O₂ batteries is urgently desirable to meet the high energy density requirements of next-generation flexible electronic devices. However, as still in infant stage, it is still very challenging to develop a high performance conventional Li–O₂ battery, to say nothing for flexible and foldable ones.

Chinese brush painting and writing is an ancient art form that developed in China hundreds of years ago and continues to fascinate contemporary artists all over the world. Inspired by the fact that the main component of painting ink is carbon and the paper is composed of fibre and thus could be flexible and inexpensive,^[33–37] a paper-ink cathode is prepared. Interestingly, when the obtained novel electrode is employed as both a new concept cathode and current collector to replace the conventional rigid and bulky counterparts, highly flexible Li–O₂ battery

with excellent mechanical strength and superior electrochemical performances is obtained. More importantly, based on this strategy, a foldable Li–O₂ battery pack is also assembled which greatly saves the occupation space and inevitably improves the volume energy density.

Figure 1a shows a schematic of a facile strategy for fabricating a flexible air cathode. Briefly, the brush is first dipped into an ink and then drawn on commonly used paper. Though various characters/patterns can be drawn, as a proof-of-concept experiment, we only draw rectangles with various breadths in this work. Due to the different loading and distribution of active material on each rectangle, theoretically, the output energy/power density could thus be tuned (Figure S1, Supporting Information). After drawing, a quick wetting of the ink can be observed due to the unique dynamic wetting process of the paper. Finally, the drawn painting is dried in air at 120 °C and a paper-ink (PI) cathode is thus obtained. This strategy for the synthesis of a PI cathode holds many advantages: (1) the low cost of paper and ink greatly decreases the cost of the cathode compared with other conventional cathode materials (e.g., carbon nanotubes) and cathode substrates (e.g., carbon paper); (2) the synthesis method is very facile and effective, and no tedious fabricated process is needed; (3) the active material could homogeneously adsorb onto the paper skeleton without the help of any additional binder or solvent, which ensures the formation of a freestanding structure;^[38–41] (4) the integrated cathode inevitably endows the Li–O₂ battery with flexible properties. Scanning electronic microscope (SEM) images of Figure 1b reveal the macroporous structures of paper sheet which can absorb ink easily. More importantly, the flexible property of the paper sheet is retained after deposited by ink as displayed in Figure 1c. Figure 1d reveals that the ink film is composed by carbon nanoparticles with size about 50 nm and form a porous morphology, which freely absorb on paper sheet and form a freestanding cathode. This structure is in favor of the mass transfer in the process of the electrochemical reaction. Figure 1e reveals the X-ray diffraction (XRD) pattern of the obtained PI cathode and no other characteristic peaks are found except carbon peak, which demonstrates that the main material is carbon. Figure 1f shows Raman spectrum of the obtained cathode and two prominent peaks at about 1336 and 1557 cm^{−1} can be assigned to the D band and G band, respectively. The intensity ratio of band and G band (I_D/I_G) could be used to estimate the disorder degree of carbon materials.^[42] The intensity ratio in this material ($I_D/I_G = 0.87 < 1$) indicates that the number defects are low, which is helpful for increasing the stability of cathode and enhance the cycling performance of Li–O₂ batteries.^[43–45]

Q.-C. Liu, L. Li, Dr. J.-J. Xu, Z.-W. Chang,
Dr. D. Xu, Y.-B. Yin, X.-Y. Yang,
T. Liu, Prof. X.-B. Zhang
State Key Laboratory of
Rare Earth Resource Utilization
Changchun Institute of Applied Chemistry
Chinese Academy of Sciences
Changchun 130022, P. R. China
E-mail: xbzhang@ciac.ac.cn



Q.-C. Liu, L. Li, Y.-B. Yin, X.-Y. Yang, Prof. Y.-S. Jiang, Prof. J.-M. Yan
School of Materials Science and Engineering
Jilin University
Changchun 130012, P.R. China
Z.-W. Chang, T. Liu
University of Chinese Academy of Sciences
Beijing 100049, P.R. China

DOI: 10.1002/adma.201503025

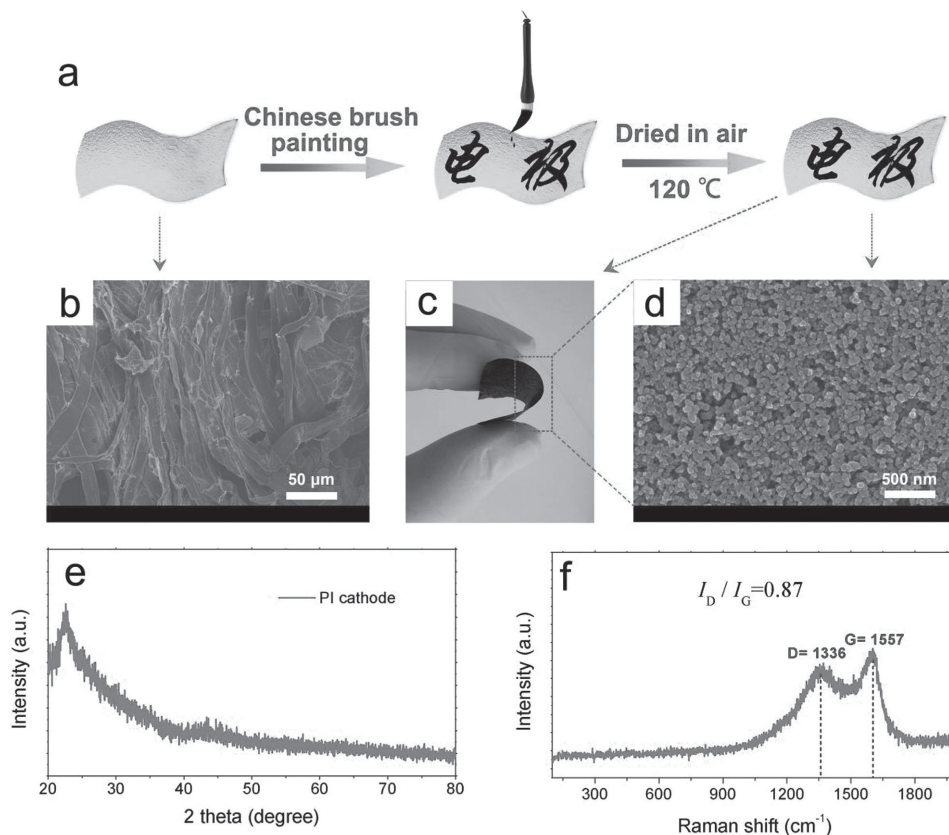


Figure 1. a) Schematic representations for the design and preparation of the PI cathode. b) SEM image of pristine paper. c) Photograph of the obtained flexible PI cathode. d) Enlarged image of (c). e) XRD pattern and f) Raman spectrum of the obtained PI cathode.

The thermal stability and the amount of absorbed electrolyte of the cathode are two key important parameters for the air cathode of Li–O₂ battery. The regeneration of the PI cathode is illustrated in Figure S2 (Supporting Information) and direct combustion test in air is applied. Firstly, ethanol is easily infiltrated into the PI cathode and found that the mass of immersed ethanol is 4–5 times of the PI cathode, which further indicates the porous structure of the PI cathode and this structure is thus favorable for mass transfer. Interestingly, the mass of PI cathode after combustion returns to the initial value, indicating the excellent thermal stability of this PI cathode. To further demonstrate the thermal stability and absorption properties, extended experiment of absorption/combustion is carried out. It can be found that even after 10th cycle, the mass of the PI cathode does not decrease and the absorption properties remained as initially. Furthermore, the mechanical stability of the PI cathode is another crucial parameter for its application in energy storage devices. As displayed in Figure S3 (Supporting Information), a stress–strain curve of the PI cathode is tested. And it is found that this PI cathode can endure strain as high as about 19 MPa. To further investigate the mechanical stability, this cathode is bended 1000 cycles and then tested its stress–strain curve. Remarkably, it is found that the mechanical strength is almost not changed. All these results demonstrate the excellent mechanical stability of the PI cathode, which would be beneficial for its electrochemical performances (vide infra).

A flexible Li–O₂ battery is then assembled as illustrated in Figure 2a, which is composed of a flexible PI cathode, glass fiber membrane, and a lithium foil as anode. It should be noted that, to exclude the possible electrochemical contributions from intercalation reactions with PI cathode, the electrochemical performance of Li–O₂ battery is first tested in pure argon atmosphere (Figure S4, Supporting Information). The discharge capacity is found to be negligible (99.4 mAh g⁻¹), demonstrating that the electrochemical capacity is derived from Li–O₂ battery reaction. Figure 2b shows that the assembled Li–O₂ battery can power commercial red LED equipment in both planar and bended conditions. As fold condition would inevitably influence the electrochemical performance, folding endurance is thus an important parameter for practical flexible device. Figure 2c displays the first discharge curves of the Li–O₂ battery with PI cathodes before and after bending 1000 cycles, wherein a high capacity of ca. 6500 mAh g⁻¹ can be obtained at a current density of 200 mA g⁻¹. Furthermore, the rate performances of the Li–O₂ batteries with these two cathodes are almost the same (Figure 2d), which is consistent with the discharge-charge profiles of Li–O₂ batteries (Figure 2e). Furthermore, the cycling performances of these two batteries with PI cathodes before and after bending 1000 cycles can still reach about 50 cycles with the capacity restricted to 1000 mAh g⁻¹ at a current density of 200 mA g⁻¹ (Figure 2f; Figure S5, Supporting Information). It should be noted that the electrochemical cycle performance is not from the flexible batteries but from the electrode.

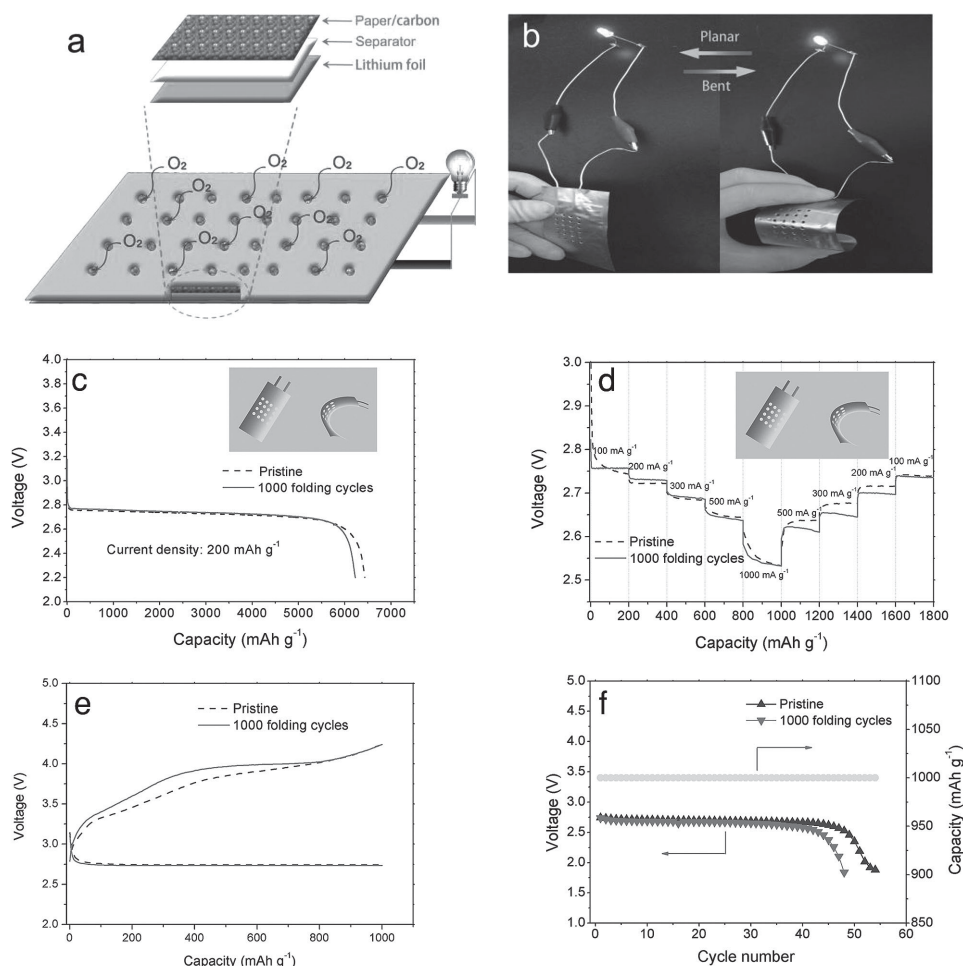


Figure 2. a) Schematic illustration of an Li–O₂ battery assembly composed of PI cathode, glass fiber (separator) and lithium foil (anode). b) Digital images of the fabricated flexible Li–O₂ battery with planar and bent conditions turning on red LED equipment. c) First discharge curves of Li–O₂ battery with the PI cathode (pristine and 1000 folding cycles) at a current density of 200 mA g^{−1}. d) Rate capability of the Li–O₂ device with the two kinds of cathodes (pristine and 1000 folding cycles) at different current densities. e) First discharge–charge curves and f) cycling performance of Li–O₂ batteries with the two kinds of cathodes (pristine and 1000 folding cycles) with a fixed capacity of 1000 mAh g^{−1}.

The morphology variation of the PI cathode is then tracked along the discharge and charge processes (Figure 3). As shown in Figure 3a, b, the pristine PI cathode is composed of carbon microspheres with an average diameter of ≈ 50 nm, forming a porous morphology (Figure 1d). After the first discharge process, toroidal products are found on the PI cathode with size about 500 nm (Figure 3c,d), which is consistent with the reported results.^[46–51] After the recharge procedure, the toroidal product is almost disappeared (Figure 3e,f), demonstrating the rechargeability of this novel PI cathode. The X-ray diffraction (XRD) technique is then employed to identify the discharge products of Li–O₂ battery with the PI cathode. Compared to the XRD pattern of the pristine cathode, new diffraction peaks at 32.9°, 35°, and 58.7° emerged (Figure 3h), which could be reasonably assigned to the (100), (101), and (110) peaks of Li₂O₂, showing that Li₂O₂ dominates the discharge product. The disappearance of Li₂O₂ peak after the subsequent charge process indicates that the decomposition of the discharge product, which demonstrates the rechargeability of this PI cathode

again. To further confirm this point, electrochemical impedance spectra (EIS) technique is then applied. As shown in Figure 3i, it is found that after the first discharge process, the impedance of the Li–O₂ cell increases significantly, which is due to the poor electronic conductivity of discharge products generated at the cathode side.^[52] Interestingly, after subsequent recharging process, the impedance of the Li–O₂ cell could almost recover its initial value, indicating that the insulated discharge products can be fully decomposed during charge process, which is consistent with the SEM images and XRD patterns discussed above, highlighting again the good rechargeability of Li–O₂ battery with PI cathode.

To further improve the electrochemical performance of the Li–O₂ battery with the PI cathode, as a proof-of-concept experiment, Ru nanoparticles are added to PI cathode (labeled PI–Ru cathode) via a simple impregnation method (Figure 4a). After immersing the PI cathode in ethanol solution containing 10×10^{-3} M RuCl₃, the obtained cathode is then dried in air and finally calcined in a tube furnace under Ar/H₂ atmosphere for

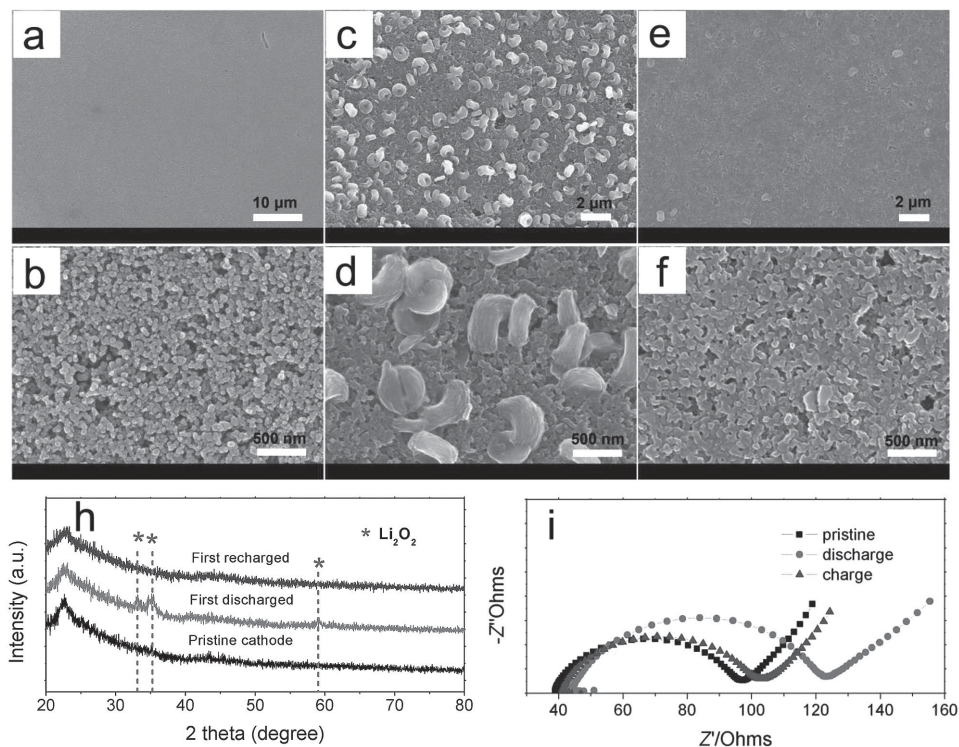


Figure 3. SEM images of the PI cathode at different stages: a,b) pristine, c,d) discharged, and e,f) recharged XRD patterns of the PI cathode at different stages (h). i) EIS of the cell with pristine, first discharge and recharge conditions.

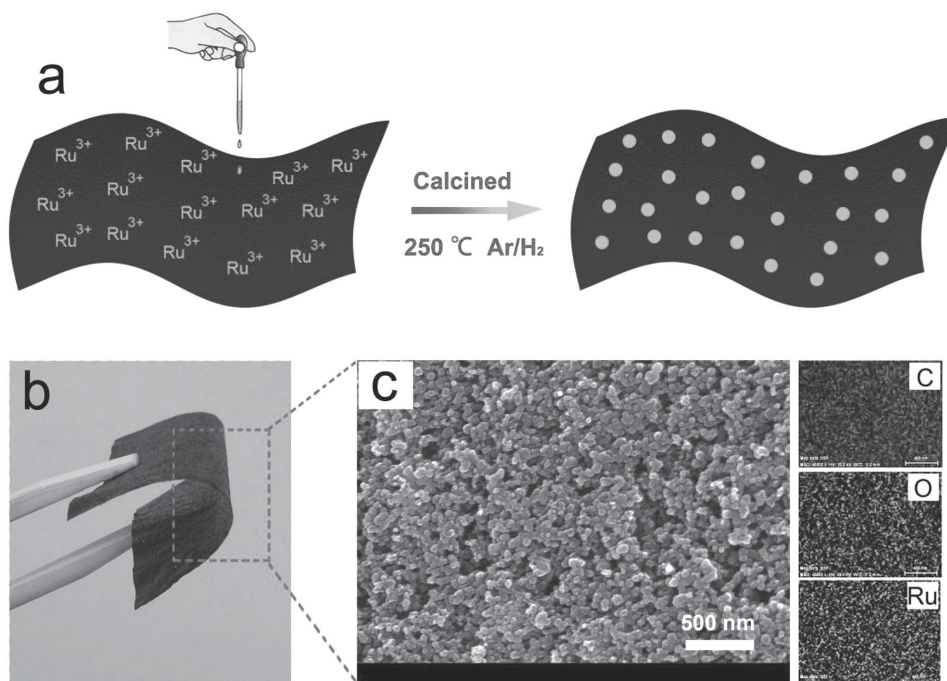


Figure 4. a) Schematic representation of the design and preparation of the PI–Ru cathode. b) Photograph of the obtained flexible PI–Ru cathode. c) SEM image of the obtained PI–Ru cathode and its corresponding EDXS maps.

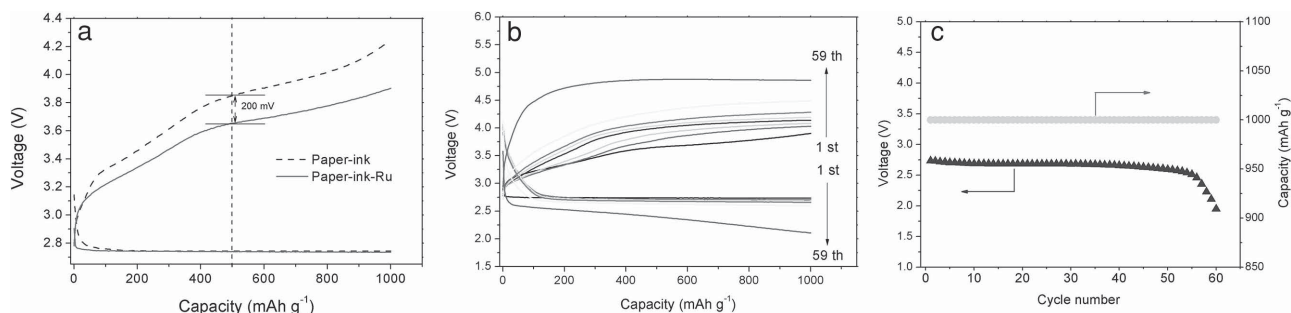


Figure 5. a) First discharge–charge curves of Li–O₂ cells with PI and PI–Ru cathodes at a fixed capacity of 1000 mAh g⁻¹. b) Discharge–charge curves of Li–O₂ cells with PI–Ru cathode and c) its corresponding cycling performance.

2 h at 250 °C. Interestingly, the as obtained PI–Ru cathode also maintains excellent flexible properties (Figure 4b). Figure 4c displays the SEM image of the obtained PI–Ru cathode, and the morphology is almost the same with that of PI cathode. Energy-dispersive X-ray spectrometry (EDXS) characterization (Figure 4c) reveals the existence and homogeneous distribution of the Ru NPs decorated on the surface of PI cathode, which also indicates that the PI–Ru cathode has been well synthesized. To verify the effect of Ru modification, electrochemical performances of Li–O₂ cells with PI–Ru cathode are displayed in Figure 5. Figure 5a displays the first discharge–charge curves of the cells with PI and PI–Ru cathodes at a current density of 200 mA g⁻¹ with a limited capacity of 1000 mAh g⁻¹. The charge voltage of the cell with PI–Ru cathode is significantly

lower than that with PI cathode by about 200 mV, showing the superior catalytic performance of Ru. Furthermore, the cycling life of the Li–O₂ cell with PI–Ru cathode can also be improved (Figure 5b,c).

Encouraged by the facile and effective fabrication strategy, a foldable Li–O₂ battery pack is fabricated for the first time (Figure 6). Figure 6a schematically shows the fabrication and work of foldable Li–O₂ battery pack. This proof-of-concept of Li–O₂ battery pack also demonstrates two unique properties compared to conventional Li–O₂ battery: (1) the inexpensive flexible paper has been served as substrate of cathode, separator as well as the outer package, and thus the assembled battery can be foldable and bendable; (2) the lithium anodes wrapped into the paper could be shared by two cathodes, which can

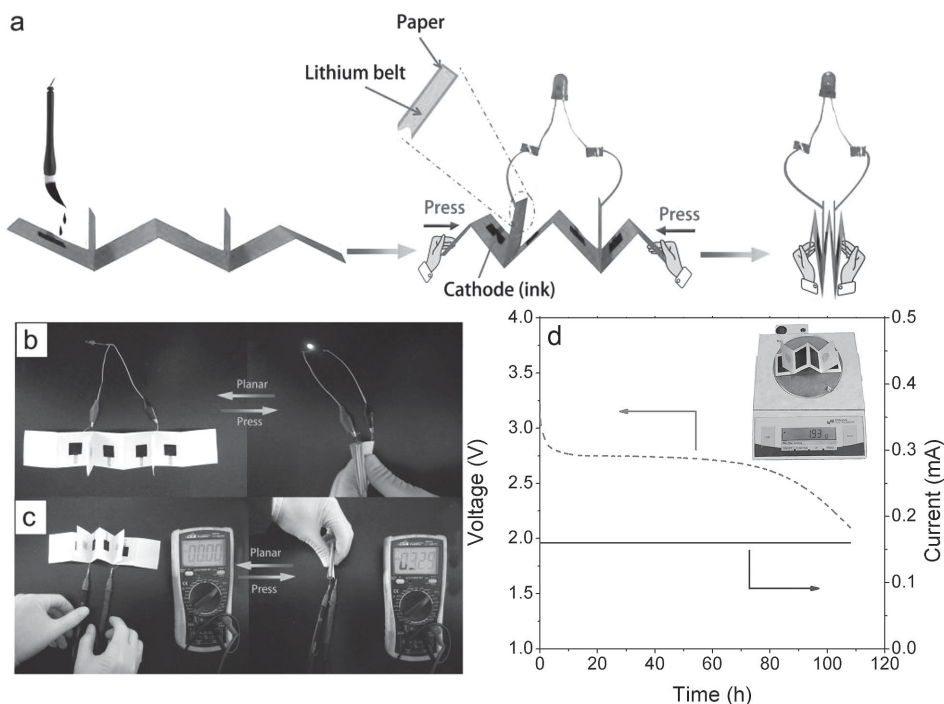


Figure 6. a) Schematic of the fabrication and working mechanism of a foldable Li–O₂ battery pack. b) Photograph of a foldable Li–O₂ battery pack turning on a red LED. c) Open-circuit voltage of this battery packs. d) Discharge voltage versus time and discharge current versus time, inset is the mass of the assembled foldable Li–O₂ battery pack.

effectively improve the utilization of lithium metal anode and reduce the total mass of this battery. These two advantages could improve both the mass energy density and volume energy density. Significantly, the feasibility of the practical application of this battery pack has also been demonstrated (Figure 6b,c; Videos S1 and S2, Supporting Information). Simultaneously, this lightweight battery pack can also be operated normally as shown in Figure 6d.

In summary, we propose and demonstrate a facile, effective and scalable strategy to fabricate a flexible and freestanding cathode for Li–O₂ batteries. When used in Li–O₂ batteries, a novel flexible Li–O₂ battery is successfully fabricated that demonstrates excellent mechanical strength and superior electrochemical performance. More importantly, a foldable Li–O₂ battery pack consisting of several paralleled cells is also successfully assembled, which effectively improves both the mass energy density and volume energy density of the Li–O₂ battery. Undoubtedly, the proposed fabrication strategy of flexible cathodes with lightweight and cheap materials (ink and the commonly used paper), and the design of flexible Li–O₂ battery (packs) have demonstrated their feasibility in the Li–O₂ field, which would also be easily extended to other important energy storage and conversion devices.

Supporting Information

Supporting Information is available from the Wiley Online Library or from the author.

Acknowledgements

This work was financially supported by the 100 Talents Programme of The Chinese Academy of Sciences, National Program on Key Basic Research Project of China (973 Program, Grant Nos. 2012CB215500 and 2014CB932300), and the National Natural Science Foundation of China (Grant Nos. 21101147 and 21203176).

Received: June 23, 2015

Revised: August 20, 2015

Published online: October 30, 2015

- [1] L. Hu, Y. Cui, *Energy Environ. Sci.* **2012**, *5*, 6423.
- [2] J. A. Rogers, T. Someya, Y. G. Huang, *Science* **2010**, *327*, 1603.
- [3] L. Li, L. Z. Wu, S. Yuan, X. Zhang, *Energy Environ. Sci.* **2014**, *7*, 2101.
- [4] M. F. L. De Volder, S. H. Tawfik, R. H. Baughman, A. J. Hart, *Science* **2013**, *339*, 535.
- [5] G. Zhou, F. Li, H. H. Cheng, *Energy Environ. Sci.* **2014**, *7*, 1307.
- [6] X. Wang, X. Lu, B. Liu, D. Chen, Y. Tong, G. Shen, *Adv. Mater.* **2014**, *26*, 4763.
- [7] Z. K. Liu, J. H. Li, F. Yan, *Adv. Mater.* **2013**, *25*, 4296.
- [8] D. J. Lipomi, B. C.-K. Tee, M. Vosgueritchian, Z. N. Bao, *Adv. Mater.* **2011**, *23*, 1771.
- [9] M. Kaltenbrunner, M. S. White, E. D. Głowacki, T. Sekitani, T. Someya, N. S. Sariciftci, S. Bauer, *Nat. Commun.* **2012**, *3*, 770.
- [10] Y. H. Lee, J. S. Kim, J. Noh, I. Lee, H. J. Kim, S. Choi, J. Seo, S. Jeon, T. S. Kim, J. Y. Lee, J. W. Choi, *Nano Lett.* **2013**, *13*, 5753.
- [11] B. Liu, J. Zhang, X. F. Wang, G. Chen, D. Chen, C. W. Zhou, G. Z. Shen, *Nano Lett.* **2012**, *12*, 3005.
- [12] S. Xu, Y. Zhang, J. Cho, J. Lee, X. Huang, L. Jia, J. A. Fan, Y. Su, J. Su, H. Zhang, H. Cheng, B. Lu, C. Yu, C. Chuang, T.-i. Kim, T. Song, K. Shigetani, S. Kang, C. Dagdeviren, I. Petrov, P. V. Braun, Y. Huang, U. Paik, J. A. Rogers, *Nat. Commun.* **2013**, *4*, 1543.
- [13] K.-H. Choi, S.-J. Cho, S.-H. Kim, Y. H. Kwon, J. Y. Kim, S.-Y. Lee, *Adv. Funct. Mater.* **2014**, *24*, 44.
- [14] Y. N. Meng, Y. Zhao, C. G. Hu, H. H. Cheng, Y. Hu, Z. P. Zhang, G. Q. Shi, L. T. Qu, *Adv. Mater.* **2013**, *25*, 2326.
- [15] L.-F. Chen, Z.-H. Huang, H.-W. Liang, Q.-F. Guan, S.-H. Yu, *Adv. Mater.* **2013**, *25*, 4746.
- [16] N. S. Liu, W. Z. Ma, J. Y. Tao, X. H. Zhang, J. Su, L. Y. Li, C. X. Yang, Y. H. Gao, D. Golberg, Y. Bando, *Adv. Mater.* **2013**, *25*, 4925.
- [17] W. Gao, N. Singh, L. Song, Z. Liu, A. L. M. Reddy, L. Ci, R. Vajtai, Q. Zhang, B. Q. Wei, P. M. Ajayan, *Nat. Nanotechnol.* **2011**, *6*, 496.
- [18] Y. N. Meng, K. Wang, Y. J. Zhang, Z. X. Wei, *Adv. Mater.* **2013**, *25*, 6985.
- [19] X. H. Lu, M. H. Yu, G. M. Wang, T. Zhai, S. L. Xie, Y. C. Ling, Y. X. Tong, Y. Li, *Adv. Mater.* **2013**, *25*, 267.
- [20] X. H. Lu, T. Zhai, X. H. Zhang, Y. Q. Shen, L. Y. Yuan, B. Hu, L. Gong, J. Chen, Y. H. Gao, J. Zhou, Y. X. Tong, Z. L. Wang, *Adv. Mater.* **2012**, *24*, 938.
- [21] G. Girishkumar, B. McCloskey, A. C. Luntz, S. Swanson, W. Wilcke, *J. Phys. Chem. Lett.* **2010**, *1*, 2193.
- [22] F. J. Li, T. Zhang, H. S. Zhou, *Energy Environ. Sci.* **2013**, *6*, 1125.
- [23] P. G. Bruce, S. A. Freunberger, L. J. Hardwick, J. M. Tarascon, *Nat. Mater.* **2012**, *11*, 19.
- [24] Y. C. Lu, B. M. Gallant, D. G. Kwabi, J. R. Harding, R. R. Mitchell, M. S. Whittingham, Y. Shao-Horn, *Energy Environ. Sci.* **2013**, *6*, 750.
- [25] S. H. Oh, L. F. Nazar, *Adv. Energy Mater.* **2012**, *2*, 903.
- [26] Z. L. Wang, D. Xu, J. J. Xu, X. B. Zhang, *Chem. Soc. Rev.* **2014**, *43*, 7746.
- [27] B. Sun, X. Huang, S. Chen, P. Munroe, G. Wang, *Nano Lett.* **2014**, *14*, 3145.
- [28] J. Liu, M. N. Banis, Q. Sun, A. Lushington, R. Li, T. K. Sham, X. Sun, *Adv. Mater.* **2014**, *26*, 6358.
- [29] L. Zhao, X. Yu, J. Yu, Y. Zhou, S. N. Ehrlich, Y.-S. Hu, D. Su, H. Li, X.-Q. Yang, L. Chen, *Adv. Funct. Mater.* **2014**, *24*, 5557.
- [30] L. Shen, E. Uchaker, X. Zhang, G. Cao, *Adv. Mater.* **2012**, *24*, 6502.
- [31] W. Ai, Z. M. Luo, J. Jiang, J. H. Zhu, Z. Z. Du, Z. X. Fan, L. H. Xie, H. Zhang, W. Huang, T. Yu, *Adv. Mater.* **2014**, *26*, 6186.
- [32] F. X. Ma, H. Hu, H. B. Wu, C. Y. Xu, Z. C. Xu, L. Zhen, X. W. Lou, *Adv. Mater.* **2015**, *27*, 4097.
- [33] J. C. Roberts, *The Chemistry of Paper*, The Royal Society of Chemistry, Cambridge **1996**.
- [34] A. W. Martinez, S. T. Phillips, G. M. Whitesides, *Proc. Natl. Acad. Sci. USA* **2008**, *105*, 19606.
- [35] E. Carrilho, A. W. Martinez, G. M. Whitesides, *Anal. Chem.* **2009**, *81*, 7091.
- [36] L. B. Hu, M. Pasta, F. La Mantia, L. F. Cui, S. Jeong, H. D. Deshazer, J. W. Choi, S. M. Han, Y. Cui, *Nano Lett.* **2010**, *10*, 708.
- [37] Q. Cheng, Z. M. Song, T. Ma, B. B. Smith, R. Tang, H. Yu, H. Q. Jiang, C. K. Chan, *Nano Lett.* **2013**, *13*, 4969.
- [38] J.-J. Xu, Z.-L. Wang, D. Xu, L.-L. Zhang, X.-B. Zhang, *Nat. Commun.* **2013**, *4*, 2438.
- [39] Z. Peng, S. A. Freunberger, Y. Chen, P. G. Bruce, *Science* **2012**, *337*, 563.
- [40] Z.-L. Wang, D. Xu, J.-J. Xu, L.-L. Zhang, X.-B. Zhang, *Adv. Funct. Mater.* **2012**, *22*, 3699.
- [41] H.-D. Lim, K.-Y. Park, H. Song, E. Y. Jang, H. Gwon, J. Kim, Y. H. Kim, M. D. Lima, R. O. Robles, X. Lepró, R. H. Baughman, K. Kang, *Adv. Mater.* **2013**, *25*, 1348.
- [42] J. P. Paraknowitsch, J. Zhang, D. Su, A. Thomas, M. Antonietti, *Adv. Mater.* **2010**, *22*, 87.
- [43] Z. Jian, P. Liu, F. Li, P. He, X. Guo, M. Chen, H. Zhou, *Angew. Chem.* **2014**, *126*, 452.

- [44] B. McCloskey, A. Speidel, R. Scheffler, D. Miller, V. Viswanathan, J. Hummelshøj, J. Nørskov, A. Luntz, *J. Phys. Chem. Lett.* **2012**, *3*, 997.
- [45] M. M. Ottakam Thotiyil, S. A. Freunberger, Z. Peng, P. G. Bruce, *J. Am. Chem. Soc.* **2012**, *135*, 494.
- [46] B. D. Adams, C. Radtke, R. Black, M. L. Trudeau, K. Zaghib, L. F. Nazar, *Energy Environ. Sci.* **2013**, *6*, 1772.
- [47] Y.-C. Lu, D. G. Kwabi, K. P. C. Yao, J. R. Harding, J. Zhou, L. Zuin, Y. Shao-Horn, *Energy Environ. Sci.* **2011**, *4*, 2999.
- [48] R. R. Mitchell, B. M. Gallant, Y. Shao-Horn, C. V. Thompson, *J. Phys. Chem. Lett.* **2013**, *4*, 1060.
- [49] E. Yilmaz, C. Yogi, K. Yamanaka, T. Ohta, H. R. Byon, *Nano Lett.* **2013**, *13*, 4679.
- [50] R. Black, J. H. Lee, B. Adams, C. A. Mims, L. F. Nazar, *Angew. Chem., Int. Ed.* **2013**, *52*, 392.
- [51] R. Black, S. H. Oh, J. H. Lee, T. Yim, B. Adams, L. F. Nazar, *J. Am. Chem. Soc.* **2012**, *134*, 2902.
- [52] Y. M. Cui, Z. Y. Wen, Y. Liu, *Energy Environ. Sci.* **2011**, *4*, 4727.
-